Thermochimica Acta 516 (2011) 40–45

Contents lists available at ScienceDirect

Thermochimica Acta

journal homepage: www.elsevier.com/locate/tca

Influence of Ni substitution on redox properties of $In_{2(1-x)}$ $Ni_{2x}TiO_{5-\delta}$ oxides

A.M. Banerjee[a], M.R. Pai[a], Jagannath[b], S.R. Bharadwaj[a,*]

[a] Chemistry Division, Bhabha Atomic Research Centre, Trombay, Mumbai 400085, India
[b] Technical Physics Division, Bhabha Atomic Research Centre, Trombay, Mumbai 400085, India

ARTICLE INFO

Article history:
Received 13 August 2010
Received in revised form
15 December 2010
Accepted 7 January 2011
Available online 18 January 2011

Keywords:
Temperature programmed reduction
Reducibility
Alloy
Hydrogen spillover
XPS

ABSTRACT

The thermal behavior of mixed metal oxides with nominal compositions of $In_{2(1-x)}Ni_{2x}TiO_{5-\delta}$ where $0.0 \le x \le 0.2$, were investigated by recording their temperature programmed reduction (TPR). The samples were synthesized by ceramic route and analyzed for phase composition using powder X-ray diffraction. The TPR profile of pristine In_2TiO_5 indicated the reduction of In^{3+}, which takes place predominantly over the other species Ti^{4+} in In_2TiO_5 sample. Ni substitution at In^{3+} site induced ease in reducibility as indicated by lowering of onset reduction temperature and T_{max}. Moreover, it also facilitated the reduction of otherwise non reducible cation, Ti^{4+}. Ni metal initially formed by reduction, dissociates and activates hydrogen which then reacts and reduces the oxide (even Ti^{4+}), a case of hydrogen spillover. The metallic Ni forms an alloy Ti_2Ni with reduced Ti metal and δIn_3Ni_2 alloy with the reduced In metal as evident by XRD and XPS results of the reduced residue of 20% Ni doped ($In_{1.6}Ni_{0.4}TiO_{5-\delta}$) sample. Due to formation of new alloy phases of δIn_3Ni_2 and Ti_2Ni, the rate of hydrogen adsorption diminishes which slows down further hydrogen activation and consequent further Ti^{4+} reduction.

1. Introduction

The physico-chemical properties of ceramic ternary oxides ($A_xB_yO_z$) having perovskites, spinel or any other structure have been investigated in great detail both because of fundamental scientific knowledge and its widespread technological applications in various fields. Specifically the ternary oxide that arise when one of the cation is titanium are titantes which are high performance materials having applications in various fields. Some of the recent applications include catalysts [1–3], sensors and actuators [4,5], solar cells [6] SOFC materials [7] and so on. So, it is imperative to study their interesting physicochemical properties the knowledge of which finds them utilized in suitable applications.

One of the interesting applications of these titanates is as catalyst for various reactions. The important considerations in designing an oxide catalyst are its thermal, chemical stability, reducibility and oxidizability [8–13]. The thermal and chemical stability and redox behavior of these titanates would play a vital role in determining their catalytic properties. Further, it is well known that substitution by transition metal cations at A or B sites of these oxide systems, further tailor their physicochemical properties which in turn results in modified catalytic behavior.

So, with the objective to study the thermal and reduction behaviors of certain titania and indium oxide based single phased compositions, which can serve as prospective catalyst for redox reactions and as photocatalysts particularly for water splitting reactions, studies have recently been taken up in our laboratories on $In_2O_3–TiO_2$ system resulting in formation of indium titanate, In_2TiO_5. The thermo-physical characteristics and redox behavior of In–Ti–O system was monitored. The catalytic properties of many titanates have been shown to be dependent on their physicochemical properties and the thermal properties of some titanates have been investigated [14–16]. We have also investigated the redox properties of Fe-doped lanthanum titanates ($La_2Ti_{2(1-x)}Fe_{2x}O_{7-\delta}$, $0.0 \le x \le 1.0$) and correlated its thermophysical properties with catalytic activity for $CO + N_2O$ reaction [17,18]. The crystal structure and luminescent properties of indium titanate oxide, In_2TiO_5 have been reported [19]. The structure of In_2TiO_5, belongs unambiguously to In_2VO_5 type. The two independent In^{3+} ions are octahedrally coordinated with six oxygen atoms, resulting in InO_6 octahedra, which by edge sharing forms infinite ribbons. Three corner connected $(In_2O_4)_n{}^{2n-}$ infinite ribbons forms the tunnels where O–Ti–O–Ti–O chains are inserted. In each tunnel formed by four ribbons one finds two chains of TiO_5 distorted square pyramids oppositely oriented. In order to perturb this structure and to modify catalytic properties, in the present study, an aliovalent substitution by transition metal Ni^{2+} at A-site was attempted, introducing thereby some micro-structural changes in the lattice. It

---

* Corresponding author at: Fuel Cell Materials and Catalysis Section, 3-193 H, Chemistry Division, Modular Labs, Bhabha Atomic Research Centre, Mumbai 400085, India. Tel.: +91 22 25595100; fax: +91 22 25505151.
E-mail addresses: shyamala@barc.gov.in, shyamala@apsara.barc.ernet.in (S.R. Bharadwaj).

0040-6031/$ – see front matter © 2011 Elsevier B.V. All rights reserved.
doi:10.1016/j.tca.2011.01.009

is apparent that the substitution of a smaller lower-valent Ni^{2+} ion (ionic radius = 0.69 Å) in place of In^{3+} (ionic radius = 0.81 Å) is likely to form an anion deficient solid solution with partial loss of oxygen in the lattice (δ).Recently we have studied the effect of B-site (Ti^{4+}) substitution by Fe^{3+} (ionic radius = 0.64 Å) and Cr^{3+} (ionic radius = 0.063 Å) on thermal properties and reduction behavior of In_2TiO_5. $In_2Ti_{1-x}Fe_xO_{5-\delta}$ and $In_2Ti_{1-x}Cr_xO_{5-\delta}$ ($0.0 \le x \le 0.2$) compositions were prepared by solid state route and the effect of substitution on redox behavior was reported [20]. In the present study, we report the A-site substitution-induced effects on indium titanate. For this purpose, $In_{2(1-x)}Ni_{2x}TiO_{5-\delta}$ ($0.0 \le x \le 0.2$) mixed oxide catalysts were synthesized using solid-state reaction and characterized by powder X-ray diffraction (XRD). The thermal and reduction behaviors were studied by recording thermogravimetric (TG), and temperature-programmed reduction (TPR) profiles. The chemical oxidation states of individual metal ions of multi-component oxides after reduction were identified using XRD and X-ray photoelectron spectroscopy (XPS).

2. Experimental

Mixed oxides with nominal composition, $In_{2(1-x)}Ni_{2x}TiO_{5-\delta}$ for $0.0 \le x \le 0.2$, were synthesized through ceramic route by mixing reactant oxides in appropriate stoichiometry as depicted by following equation:

$$(1-x)In_2O_3 + TiO_2 + 2xNIO \rightarrow In_{2(1-x)}Ni_{2x}TiO_{5-\delta}$$

The pellets of homogeneous mixtures were calcined at 900 °C for 24 h, 1000 °C for 24 h and finally at 1250 °C for 12 h, with intermittent grindings so as to ensure the uniformity and the completion of the reaction.

The powder XRD patterns were recorded on a Philips X-ray diffractometer (model PW 1710), equipped with a graphite monochromator and Ni-filtered Cu Kα radiation.

The thermal behavior of these samples (~20 mg) was monitored by recording their TG profiles both in air and 5% H_2 + Ar atmospheres, in the temperature range of 25–1000 °C at a heating rate of 10 °C min^{-1} on Setaram TGA-92 instrument.

Redox behavior of catalyst was studied by recording temperature programmed reduction/oxidation (TPR/TPO) profiles on a TPDRO-1100 analyzer (ThermoQuest, Italy) in temperature range of 25–1100 °C under the flow of H_2 (5%) + Ar, gas mixtures at a flow rate of 20 ml min^{-1}, with a heating rate of 6 K min^{-1}. The samples were pretreated at 350 °C for about 2.5 h in helium, prior to recording of the first TPR run. A thermal conductivity detector (TCD) is employed to monitor the change in composition of reactive gas mixture with time. The water formed during reduction process was removed from the flowing gas by the help of a soda lime trap placed just before the detector. Hence the signal obtained was primarily due to change in thermal conductivity of the flowing gas by consumption of hydrogen. The amount of hydrogen consumed by the sample during a TPR run corresponded to the area under the TPR profile. The calibration factor (μmoles of H_2 per mV of TCD signal) for the H_2 was calculated using the standard sample. This factor has been employed in all the substituted samples and the experimental amount of H_2 consumed was obtained. The calculated value of H_2 consumed by the sample was compared with the experimental value.

XPS studies were carried out on electron spectrometer using Mg Kα X-rays ($h\nu$ = 1253.6 eV) as the primary source of radiation. The appropriate corrections for charging effect were made with the help of a C 1s signal appearing at 285.1 eV.

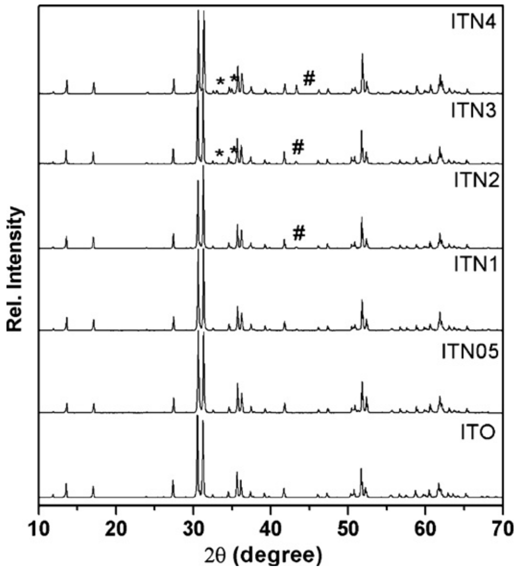

Fig. 1. XRD patterns of $In_{2(1-x)}Ni_{2x}TiO_{5-\delta}$ samples, # indicates peaks due to unreacted NiO phase and * indicates the peaks arising from $NiTiO_3$ phase.

3. Results

3.1. XRD

Table 1 lists the abbreviations and phases identified from XRD patterns of all the $In_{2(1-x)}Ni_{2x}TiO_{5-\delta}$ ($0.0 \le x \le 0.2$) samples prepared by solid state method. Fig. 1 shows the powder XRD patterns of In_2TiO_5 and corresponding patterns observed due to aliovalent substitution of Ni^{2+} in place of In^{3+} at A-site. From Fig. 1, it is observed that the XRD pattern of $x = 0$, composition matches well with that of orthorhombic In_2TiO_5 (JCPDS card No. 30-0640) oxide. The lines due to reactant oxides are missing in these patterns thus confirming the completion of the solid-state reaction. In_2TiO_5 is isostructural with In_2VO_5. It crystallizes in the orthorhombic space group, with a = 0.7241 nm, b = 0.3427 nm, c = 1.4878 nm, cell volume = 0.3692 nm^3 and Z = 4. The XRD patterns of ITN05 ($In_{1.95}Ni_{0.05}TiO_{5-\delta}$) and ITN01 ($In_{1.9}Ni_{0.1}TiO_{5-\delta}$) compositions match with the XRD patterns of unsubstituted indium titanate sample as shown in Fig. 1. Thus, lower extent of Ni substitution resulted in single phase material comprised of In_2TiO_5 phase due to formation of solid solution of Ni with the lattice of the parent compound. But for samples having Ni content $x \ge 0.1$ in $In_{2(1-x)}Ni_{2x}TiO_{5-\delta}$ a very low intensity line (marked with #) was observed which corresponds to the 100% peak of NiO (JCPDS card No. 47-1049). Thus for these compositions in addition to parent phase there was segregation of unreacted NiO phase in very small proportion. Moreover, for samples having higher Ni content i.e. $x \ge 0.15$, a third phase of $NiTiO_3$ (JCPDS card No. 33-0960, peaks marked with *) was observed in addition to the unreacted nickel oxide phase (Fig. 1). This phenomenon of segregation of secondary phases in the Ni doped samples can be attributed to the large difference in ionic radii between the substituent cation Ni (0.069 Å) and the parent cation In (0.081 Å).

3.2. Temperature programmed reduction behavior (TPR)

The typical first temperature programmed cycle (TPR) of substituted samples and unsubstituted sample are shown in Fig. 2. The TPR profile of unsubstituted, In_2TiO_5 sample as seen in Fig. 2 comprises of a prominent band with onset at ~625 °C and extending beyond 1000 °C. This indicated the predominant reduction of one of the species, identified to be In^{3+}, in the temperature range of

Table 1
Identification of phase in $In_{2(1-x)}Ni_{2x}TiO_{5-\delta}$ ($0.0 \leq x \leq 0.2$) samples and their abbreviations.

S. no.	Nominal Composition	Ni content (2*x*)	Abbreviation	Phase identification by XRD
1	In_2TiO_5	0.00	ITO	Single phase, In_2TiO_5
2	$In_{1.95}Ni_{0.05}TiO_{5-\delta}$	0.05	ITN05	Single phase, In_2TiO_5
3	$In_{1.9}Ni_{0.1}TiO_{5-\delta}$	0.1	ITN1	Single phase, In_2TiO_5
4	$In_{1.8}Ni_{0.2}TiO_{5-\delta}$	0.2	ITN2	In_2TiO_5 and NiO
5	$In_{1.7}Ni_{0.3}TiO_{5-\delta}$	0.3	ITN3	In_2TiO_5, NiO and $NiTiO_3$
6	$In_{1.6}Ni_{0.4}TiO_{5-\delta}$	0.4	ITN4	In_2TiO_5, NiO and $NiTiO_3$

600–1100 °C over other reducible species in In_2TiO_5 sample. The temperature maximum (T_{max}) of the reduction bands corresponds to ~1070 °C. However, Ni^{2+} substitution at In^{3+} site has induced considerable changes in the reduction profile of indium titanate. In case of compositions having higher content of Ni, viz., ITN2 and ITN4 TPR profiles (Fig. 2), exhibit two-three weak bands in low temperature range of 450-800 °C in addition to main reduction band. The presence of these bands is probably attributed to reduction of $Ni^{2+} \rightarrow Ni^0$ along with reduction of In^{3+}. At the same time, the T_{max} of the individual peaks was found to be lower in the case of substituted samples. For instance, we observe the lowering of T_{max} around by 80 °C for ITN4 in Fig. 2, as compared to the TPR profile of an unsubstituted phase. Also the onset reduction temperature of 625 °C in unsubstituted phase has considerably decreased by Ni substitution as shown in Fig. 2. The TPR profile as a whole has shifted to lower temperature as a result of Ni substitution. These results are comparable to our earlier work [20] where Fe and Cr substituted at B-site were found to increase the reducibility of indium titanate. Thus, M (Ni^{2+}, Cr^{3+} and Fe^{3+}) substitution has undoubtedly facilitated the reduction of In_2TiO_5 phase. These changes in the TPR profiles can be ascribed to the nonstoichiometry and imperfections generated in the single phased compositions as a result of A and B-site substitution.

3.3. Thermo gravimetric studies

Both substituted and unsubstituted samples did not show any weight loss in TG when recorded in O_2 (5%) + Ar, thus indicating that all substituted $In_{2(1-x)}Ni_{2x}TiO_{5-\delta}$ oxide samples are stable in air up to 1000 °C. Thus indicating that all $In_{2(1-x)}Ni_{2x}TiO_{5-\delta}$ ($x = 0.0$–0.4) samples once formed, do not pick up either moisture or CO_2, and are thermally stable compositions till 1000 °C. Although, in O_2 (5%) + Ar atmosphere these compositions are stable whereas in H_2 (5%) + Ar, the corresponding TG exhibits substantial weight loss. A representative TG-DTA plot of ITN4 in H_2 (5%) + Ar atmosphere is shown in Fig. 3. The weight loss in TG plot starts above ~500 °C and continues up to ~1050 °C in the 20% Ni-substituted sample. As revealed by temperature programmed reduction profiles (Fig. 2) of these oxides, we can infer that this weight loss is due to reduction of these oxides in H_2 atmosphere. Mainly the weight loss is attributed to reduction of species, In^{3+} and Ni^{2+}, to In^0 and Ni^0 respectively. The evidence of the above inference comes from temperature programmed reduction profiles of In_2O_3 and TiO_2 oxides. TPR profiles of In_2O_3 and TiO_2 reactant oxides (exhibited as inset in Fig. 3) suggests that In^{3+} species reduces above 600 °C with T_{max} at 670 °C, whereas TiO_2 does not reduce up to 1000 °C recorded in the range of 25–1000 °C under H_2 flow (5% H_2 in Ar).

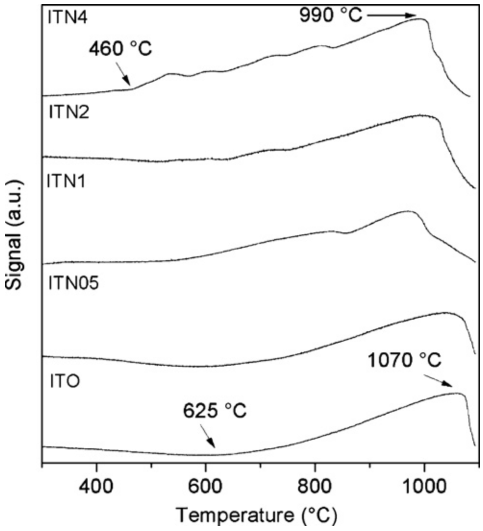

Fig. 2. Typical first TPR cycle of $In_{2(1-x)}Ni_{2x}TiO_{5-\delta}$ samples as a function of x.

3.4. Ex situ characterization of reduced residue samples

3.4.1. XRD

Fig. 4 shows the XRD patterns of reduced residue of In_2TiO_5, ITN2 and ITN4 samples obtained after recording TPR. In the reduced In_2TiO_5 and ITN2 samples the presence of prominent lines at $2\theta = 32{\cdot}98°$, 39·2° conforms to reported pattern of In^0 (JC-PDS No.05-0642). Other strong lines at 27.44°, 36.08° and 54.32° match well with rutile TiO_2 phase (JC-PDS No. 21-1276). Thus, both metallic indium and rutile titania were present in these two reduced samples. There was no other phases present in the reduced In_2TiO_5 sample. No prominent additional lines were also observed in the reduced ITN2 sample, except for a weak hump at 41.2°. This peak can be attributed to the formation of an alloy of Ni and In namely δIn_3Ni_2 (JCPDS No. 070298). The small amount of nickel present

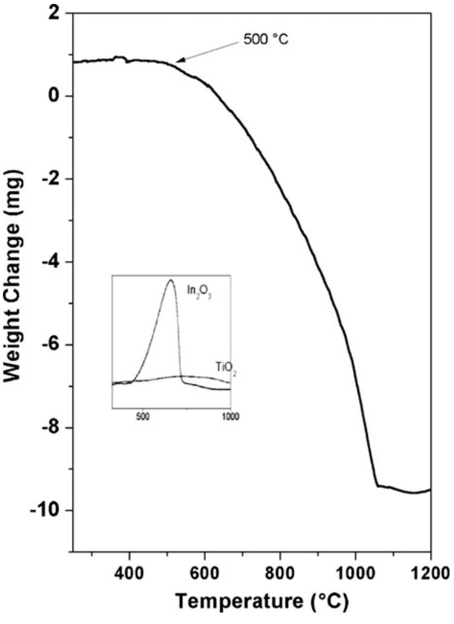

Fig. 3. Thermogram plot of ITN4 composition recorded in H_2 (5%) + Ar atmosphere. Inset exhibiting TPR profiles of In_2O_3 and TiO_2.

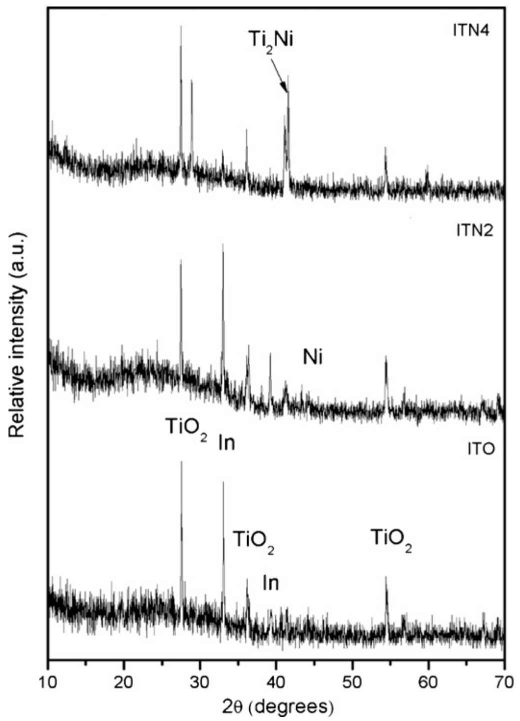

Fig. 4. XRD patterns of spent $In_{2(1-x)}Ni_{2x}TiO_{5-\delta}$ samples after recording TPR in H_2 (5%) + Ar atmosphere of ITO ITN2 and ITN4 compositions. The peaks due to δIn_3Ni_2 alloy are marked by *.

in the sample was initially reduced at a lower temperature with an onset at ~450 °C and subsequently In^{3+} was also reduced (refer Fig. 2). The reduced metallic nickel then reacted with the reduced In metal to form the In-Ni alloy. An interesting feature was observed in the XRD pattern of reduced ITN4 sample. The intensity of the peaks due to reduced Indium metal was reduced drastically, along with the appearance of prominent lines (marked by *) at $2\theta = 28.9$, 41.0, 41.3 and 59.8. These peaks are attributed to the presence of δIn_3Ni_2 phase. Remaining line in the residue were at $2\theta = 41.5°$. An alloy formation of Ni–Ti is indicated by this peak as $2\theta = 41.57°$ corresponds to 100% peak due to reflection from 511 plane of Ti_2NI alloy (JCPDS No. 180898). This suggests that Ti^{4+} an otherwise stable cation towards reduction got reduced within 1100 °C. The formation of Ni–Ti alloy on reduction of ITN4 sample is quite plausible as revealed by the XRD pattern, as secondary phase of $NiTiO_3$, also got reduced along with major indium titanate phase. This new phases possibly would have facilitated the reduction of Ti^{4+} along with reduction of Ni^{2+}. Any of the lines in the spent samples do not match with the reported XRD pattern of Ni metal alone (JC-PDS. No. 04-0850). So, Ni metal formed by reduction was very active and reacted with other reduced phases to form alloys. Further, the presence of Ni facilitated the reduction of In^{3+} as the T_{max} of the individual peaks due to reduction of In^{3+} was found to be lowered in the case of substituted samples. In addition to this, the otherwise non-reducible cation Ti^{4+} also got reduced in the 20% substituted sample which might probably be due to autocatalytic effect of Ni^{2+}. This phenomenon can be referred to as an incident of hydrogen spillover in mixed metal oxide. The Ni metal initially formed by reduction of the cation was active enough to dissociate and activate the hydrogen, which in turn could even reduce Ti^{4+} cation in addition to facilitating the reduction of In^{3+}. It could also be suggested that the extent of reduction of Ti^{4+} and subsequent alloy formation would depend on the content of secondary phase. In ITN2 sample In^{3+} was replaced partially by Ni^{2+} and the reduced Ni metal facilitated the reduction of In^{3+} cation and then an alloy formation took place. This fact is evident from the TPR curve where the whole reduction pattern including T_{max} for reduction of In^{3+} shifts to lower temperature. Further in the ITN4 sample the reduction of partially substituted Ni^{2+} cation generated Ni metal which dissociated and activated the hydrogen which eased the reduction of In^{3+} cation and also reduced Ti^{4+}. This process of reduction of Ti^{4+} if continued would have resulted in the reduction of all Ti^{4+} but the formation of the Ti_2Ni alloy prevented further hydrogen activation and that further reduction of the Ti^{4+} was hindered. So, only partial reduction of Ti^{4+} was feasible. The presence of $NiTiO_3$ phase might have assisted the above process. Thus, Ni substitution at In-site of In_2TiO_5 had a drastic effect on the reduction behavior of indium titanates. TPR results in conjunction with XRD studies reveal the reduction of $In^{3+} \rightarrow In^0$, while Ni^{2+} facilitated the reduction of otherwise non-reducible cation Ti^{4+} and resulted in formation of Ni–Ti alloy (Ti_2Ni).

3.4.2. X-ray photoelectron spectroscopy (XPS)

In Fig. 5a and b, the X-ray photoelectron (XPS) spectrum of fresh, and completely reduced ITN4, sample are shown, which were recorded in order to identify the oxidation states of indium and titanium metal ions present in the spent samples after the reduction. Table 2 lists the elements identified and their oxidation states in the fresh and reduced samples. The binding energies at 445.9 eV and 457.5 eV corresponding to In ($3d_{5/2}$) and Ti ($2p_{3/2}$) which matches with the reported binding energies for In in +3 and Ti in +4 oxidation state present in fresh ITN4 sample as shown in Fig. 5a and b. But, the binding energy at 445.9 eV as observed in the fresh sample in Fig. 5a is shifted to lower binding energies of 444.1 eV in completely reduced ITN4 sample. XPS spectra suggest the existence of indium in +3 oxidation state in the fresh sample and In(0) in completely reduced sample. The changes in oxidation states of Ti present in the fresh and reduced sample are shown in Fig. 5b.

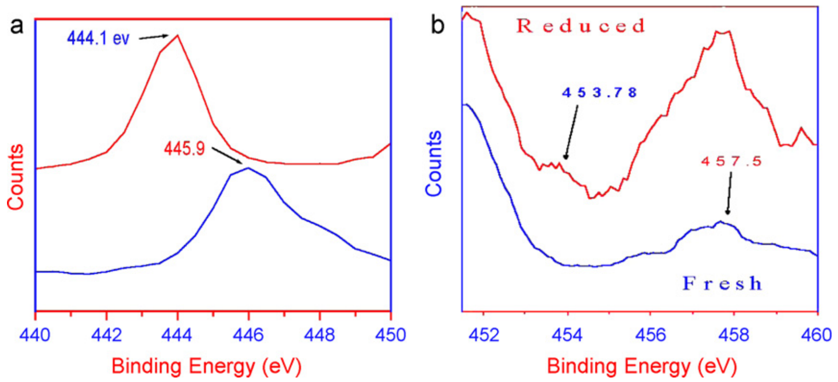

Fig. 5. Binding energies of different metal ions in partially reduced sample of ITN4 obtained after recording TPR up to 1000 °C of (a) In (3d), and (b) Ti (2p).

Table 2
Representative XPS binding energy values of different elements in ITN4 samples obtained before and after the first TPR cycle in temperature range of 25-1100 °C.

BE of XPS signal (eV)				
Before TPR			After TPR	
Elements	In $3d_{5/2}$	Ti $2P_{3/2}$	In $3d_{5/2}$	Ti $2P_{3/2}$
B.E	445.9	457.5	444.1	457.5, 453.7
Oxidation state	+3	+4	0	+4, 0
	In^{3+}	No peak due to Ti^0 metal	In^0	Ti^{4+}, Ti^0

In the reduced sample, in addition to major peak at 457.5 eV a shoulder is observed at 453.7 eV corresponding to Ti(0) state. The appearance of this shoulder peak confirms the reduction of Ti^{4+} to Ti metal during the temperature programmed reduction (TPR) experiments. In addition, in Fig. 5a, a shoulder appears at higher binding energy in the XPS spectra of Indium ion for the fresh sample, but it completely disappears in the spectra recorded after the complete reduction. The appearance of shoulder is attributed to the interaction of In^{3+} with other ions present in the compound. Thus as process of reduction proceeds, the interaction of Indium with other ions decreases or it gets segregated out from the sample. However, presence of In 1+ in the reduced sample is not observed as observed earlier for partially reduced sample in case of iron substitution [20]. Intensity of In (3d) peak is considerably increased in Fig 5a, after complete reduction as compared to fresh sample. Thus, ITN4, sample on reduction, deposits the metallic Indium on the surface and hence the peak intensity due to Indium on surface increases. It is well known that the catalytic properties of a sample are sensitive to its surface composition; therefore this observation may play a crucial role in deciding its performance for redox reactions. The XPS results in accordance with TPR and thermogravimetry results suggests the formation of metallic Ti(0) along with Ti^{4+} and In (0) when ITN4 was reduced in H_2 up to 1100 °C whereas unsubstituted In_2TiO_5 did not reveal any reduction of Ti^{4+} species. Thus presence of Ni influenced the reduction behavior of Ti^{4+} species present in the sample by activating H_2 molecules.

4. Discussion

The reduction of $In_{2(1-x)}Ni_{2x}TiO_{5-\delta}$ oxide samples is represented by following equation:

$$In_{2(1-x)}{}^{3+}Ni_{2x}{}^{2+}Ti^{4+}O_{5-\delta}(s) + (3-\delta)H_2(g) \xrightarrow{490-1100\,^{\circ}C} 2(1-x)In^0(s) + 2xNi^0(s) + Ti^{4+}O_2(s) + (3-\delta)H_2O(g)$$

H_2 consumption data calculated as well as that observed from the areas under TPR peak, for all samples for the first reduction cycle (TPR) is listed in Table 3. The comparison shows that except for ITN1 for all other samples experimental values are higher than calculated values. This discrepancy increases with increase in Ni content as observed from Table 3. It can be explained on the basis of autocatalytic reduction of the samples in the presence of Ni^{2+} cations. We have reported earlier [20] that Ti^{4+} cation was stable in H_2 up to 1000 °C in Cr and Fe substituted In_2TiO_5 samples. As such, to obtain the TPR profiles of some simple oxides, TiO_2 and Cr_2O_3, are difficult because the standard approximate free energy change (ΔG° in KJ/mol) for the process: $MO + H_2 \rightarrow metal + H_2O$ are respectively ~220 and ~140 [21]. However for $In_{2(1-x)}Ni_{2x}TiO_{5-\delta}$ samples, in addition to the normal nucleation and growth process, during reduction the presence of Ni^{2+} in even a minor amount modifies the reduction. Ni metal initially formed by reduction dissociates and activates hydrogen. This hydrogen then reacts and reduces the oxide (even Ti^{4+}). This phenomenon is termed as hydrogen spillover. In oxide catalysts the presence of metal cations, which after reduction generates the active metal that can dissociate and activate the hydrogen for facilitating an otherwise difficult reduction phenomenon. It is reported [22,23] that hydrogen spillover can be broken into three primary steps: (i) dissociative chemisorption of gaseous H_2 on a transition metal catalyst; (ii) migration of H atoms from the catalyst to the substrate and (iii) diffusion of H atoms on substrate surfaces and/or in the bulk materials. In this case the metallic Ni formed after reduction is the transition metal catalyst. The substrate is the remnant oxide from which Ni^{2+} cation gets eliminated and then the reduction of bulk In^{3+} occurs by diffusion of H-atoms into the remnant oxide material and thus the reduction profile shifts to lower temperature. Diffusion of H atoms and subsequent reduction of Ti^{4+} is definitely easier in $NiTiO_3$ that the indium titanate phase so we observe higher amount of Ti^{4+} reduction in the sample. This is further corroborated by the TPR results where we observe increased hydrogen consumption discrepancy with an increase in Ni content. Alloy formation of the transition metal catalyst Ni with In and Ti prevented further reduction of Ti^{4+} but In^{3+} being reducible was completely reduced. Such phenomenon of hydrogen spillover has been noticed over nickel metal used as catalyst in hydrogen storage materials like activated carbon, where hydrogen spillover is mainly responsible in increasing the storage capacity [24]. Recently, pioneering studies by Yang et al. revealed novel processes to store substantial quantities of hydrogen via hydrogen spillover [25–27].

5. Conclusions

A-site substitution by a divalent Ni^{2+} cation at In^{3+} site of In_2TiO_5 resulted in single phase compositions at low extent of substitution (up to 5%), biphasic at a higher substitution (10%) with very low impurity phase of unreacted NiO and triphasic at even higher Ni content (15–20%), having very low concentrations of NiO and $NiTiO_3$ phase. The temperature programmed reduction, XRD and XPS studies establishes complete reduction of In^{3+} and Ni^{2+} to In^0 and Ni^0 states in temperature range of 450–1100 °C in all the samples. Ni substitution induced considerable ease in reducibility (T_{max}) of substituted samples as compared to In_2TiO_5 phase. The substitution-induced non-stoichiometry and the microstrucural defects may cause the distortion in the lattice, thus facilitating the reduction of oxides. The interesting observation was the reduction of otherwise non-reducible cation Ti^{4+}, in the 20% substituted sample, ITN4. Ni metal initially formed by the reduction of Ni^{2+} dissociate and activate the hydrogen which eased the In^{3+} reduction and even facilitated the reduction of Ti^{4+}. Metallic Ni and In reacts to form δIn_3Ni_2 alloy while metallic Ni and Ti reacts to form an alloy Ti_2Ni. Due to the formation of these alloys the rate of hydrogen adsorption diminishes, which slows down further hydrogen activation and

Table 3
H_2 consumption data of $In_{2(1-x)}\,Ni_xTiO_{5-\delta}$ samples obtained from the first TPR cycle in temperature range of 25–1100 °C.

Sample composition[a]	Calculated	Experimental[b]	Residue as identified by XRD
In_2TiO_5	8390	8404	In^0 andTiO_2 rutile
$In_{1.95}Ni_{0.05}TiO_{5-\delta}$	8396	9009	
$In_{1.9}Ni_{0.1}TiO_{5-\delta}$	8401	8358	
$In_{1.8}Ni_{0.2}TiO_{5-\delta}$	8412	9528	In, TiO_2 and δIn_3Ni_2
$In_{1.7}Ni_{0.3}TiO_{5-\delta}$	8424	10,514	
$In_{1.6}Ni_{0.4}TiO_{5-\delta}$	8436	10,153[c]	In, TiO_2, δIn_3Ni_2 and Ti_2Ni

[a] Stoichiometry determines δ as x.

[b] TCD signal for manual injection of standard hydrogen has been used for calibration to find out the H_2 consumption.

[c] The difference observed in experimental values (higher) of H_2 consumed as compared to calculated values is attributed to reduction of Ti^{4+} metal ions to Ti metal driven by presence of Ni^{2+} ions.

this might have prevented the complete reduction of Ti^{4+} to Ti^0.

References

[1] J. Park, J. Alloys Compd. 492 (2010) L57–L60.
[2] J. Kim, D.W. Hwang, H.G. Kim, S.W. Bae, S.M. Ji, J.S. Lee, Chem. Commun. (2002) 2488–2489.
[3] W.F. Yao, X.H. Xu, H. Wang, J.T. Zhou, X.N. Yang, Y. Zhang, S.X. Shang, B.B. Huang, Appl. Catal. B: Environ. 52 (2004) 109–116.
[4] P.T. Moseley, Sens. Actuators B 6 (1992) 149–156.
[5] G.H. Jain, L.A. Patil, M.S. Wagh, D.R. Patil, S.A. Patil, D.P. Amalnerkar, Sens. Actuators B 117 (2006) 159–165.
[6] L. Zhang, H. Lin, N. Wang, C. Lin, J. Li, J. Alloys Compd. 431 (2007) 230–235.
[7] V. Vashook, L. Vasylechko, M. Knapp, H. Ullmann, U. Guth, J. Alloys Compd. 354 (2003) 13–23.
[8] M. Woodhousea, B.A. Parkinson, Chem. Soc. Rev. 38 (2009) 197–210.
[9] F. Huber, J. Walmsley, H. Venvik, A. Holmen, Appl. Catal. A: Gen. 349 (2008) 46–54.
[10] M.R. Pai, B.N. Wani, N.M. Gupta, Thermochim. Acta 425 (2005) 109–113.
[11] L.G. Tejuca, J.L.G. Fierro, Properties and Applications of Perovskite type Oxides, New York, Marcel Dekker, 1993.
[12] R.I. Slioor, J.M. Kanervo, T.J. Keskitalo, A.O.I. Krause, Appl. Catal. A: Gen. 344 (2008) 183–190.
[13] N. Jagtap, M. Bhagwat, P. Awati, V. Ramaswamy, Thermochim. Acta 427 (2005) 37–41.
[14] Z. Xu, K. Inumaru, S. Yamanaka, Appl. Catal. A: Gen. 210 (2001) 217–224.
[15] P. Rodrigues de Lucena, O. Dantas Pessoa-Neto, I.M. Garcia dos Santos, A.G. Souza, E. Longo, J.A. Varela, J. Alloys Compd. 397 (2005) 255–259.
[16] K.P. Lopes, L.S. Cavalcante, A.Z. Simoes, J.A. Varela, E. Longo, E.R. Leite, J. Alloys Compd. 468 (2009) 327–332.
[17] M.R. Pai, A.M. Banerjee, K. Kartha, R.V. Pai, V.S. Kamble, S.R. Bharadwaj, J. Phys. Chem. B 114 (20) (2010) 6943–6953.
[18] K. Kartha, M.R. Pai, A.M. Banerjee, R.V. Pai, S.S. Meena, S.R. Bharadwaj, J. Mol. Catal. A, communicated.
[19] J.P. Gaewdang, P. Chaminade, A. Gravereau, C. Garcia, P. Fouassier, Hagenmuller, R. Mahiou, Mater. Res. Bull. 28 (1993) 1051–1060.
[20] M.R. Pai, A.M. Banerjee, S.R. Bharadwaj, S.K. Kulshreshtha, J. Mater. Res. 22 (2007) 1787–1796.
[21] N.W. Hurst, S.J. Gentry, A. Jones, Catal. Rev. – Sci. Eng. 24 (2) (1982) 233–309.
[22] H. Cheng, L. Chen, A.C. Cooper, X. Sha, Guido P. Pez, Energy Environ. Sci. 1 (2008) 338–354.
[23] W. Curtis Conner Jr., John L. Falconer, Chem. Rev. 95 (1995) 759–768.
[24] M. Zielinski, R. Wojcieszak, S. Monteverdi, M. Mercy, M.M. Bettahar, Int. J. Hydrogen Energy 32 (2007) 1024–1032.
[25] H. Chen, R. T. Yang, Langmuir, doi:10.1021/la100172b.
[26] Y.W. Li, R.T. Yang, J. Phys. Chem. B 110 (2006) 17175–17181.
[27] R.T. Yang, Y. Wang, J. Am. Chem. Soc. 131 (12) (2009) 4224–4226.